Macromolecular Research, Vol. 15, No. 6, pp 491-497 (2007)

Monte Carlo Simulation of the Molecular Properties of Poly(vinyl chloride) and Poly(vinyl alcohol) Melts

Sung Doo Moon*, Young Soo Kang, and Dong J. Lee

Department of Chemistry, Pukyong University, Busan 108-737, Korea

Received December 31, 2006; Revised July 13, 2007

Abstract: NPT Monte Carlo simulations were performed to calculate the molecular properties of syndiotactic poly(vinyl chloride) (PVC) and syndiotactic poly(vinyl alcohol) (PVA) melts using the configurational bias Monte Carlo move, concerted rotation, reptation, and volume fluctuation. The density, mean square backbone end-to-end distance, mean square radius of gyration, fractional free-volume distribution, distribution of torsional angles, small molecule solubility constant, and radial distribution function of PVC at 0.1 MPa and above the glass transition temperature were calculated/measured, and those of PVA were calculated. The calculated results were compared with the corresponding experimental data and discussed. The calculated densities of PVC and PVA were smaller than the experimental values, probably due to the very low molecular weight of the model polymer used in the simulation. The fractional free-volume distribution and radial distribution function for PVC and PVA were nearly independent of temperature.

Keywords: poly(vinyl chloride), poly(vinyl alcohol), Monte Carlo simulation, concerted rotation.

Introduction

Molecular simulation has been applied to study the microscopic structure and dynamics of polymer and its mixture. These studies for PVC and PVA have mainly been performed by molecular dynamics (MD) simulation. Tanaka and Mattice[1] and Smith and co-workers[2] calculated the conformation of atactic PVC by MD simulation. Neelov and co-workers[3] reported the differences in structure and dynamical behavior of polar PVC and nonpolar PVC by MD simulation. Neyertz and co-workers[4] reported the conformational and configurational properties of PVC determined from MD simulation, and compared to those sampled for the same models by the pivot Monte Carlo (MC) simulation. van der Vegt[5] performed to calculate several solvation quantities for gas penetrants in PVC and PVA. Also MD simulations for PVA have been performed; the thermodynamic properties or microstructures of pure PVA,[6,7] the behavior water-PVA mixtures,[8-10] diffusion properties of small molecules in PVA,[11,12] and the blend compatibility of PVA with poly(methyl methacrylate).[13]

Recently, MC techniques have been developed to effectively sample the configurations. Especially the configurational bias Monte Carlo (CBMC) moves[14,15] and the concerted rotation (CONROT)[16,17] accelerate the equilibration of dense polymer. In CBMC move, the entire molecule does not move at random, but the chain molecule is grown segment by segment in such a way that regions of favorable energy are found. Pablo *et al.*[15] proposed the continuum configurational bias (CCB) MC method, which is similar to the CBMC move. The CONROT move is initiated by excising a randomly selected internal trimer of backbone atoms in chain, and the trimer is then reconstructed. And the End-bridging (EB) MC move[18,19] involves the building of the bridging trimer, which are sufficient for equilibrating a larger polymer chain. The EBMC move changes the length of chain which is controlled at equilibrium by a semi-grand canonical ensemble formalism. Karayiannis and co-workers[20,21] introduced the double-bridging and intramolecular double rebridging chain connectivity-altering MC move which entail the construction of two trimer bridges between two chosen pairs of dimers along the backbones of two different chains or along the same chain. This MC move displaces branch points along its backbone. The CONROT and EBMC move and its variants have been used for large-scale characteristic of long polymer chains such as polyethylene,[18] *trans*-polyisoprene,[22] *cis*-1,4 polyisoprene,[23] *cis*-1,4 polybutadiene and 1,2-polybutadiene.[24]

The MC simulation of polymer was not very often studied. The aim of this study is to check the MC moves for complex polymer with partial charge and to calculate the conformational, microstructural, and thermodynamic prop-

*Corresponding Author. E-mail: sdmoon@pknu.ac.kr

erties of PVC and PVA melts above the glass transition temperature. To equilibrate the polymer system, four MC moves are implemented: CONROT move, CBMC move, reptation, and volume fluctuation. In the following sections the details of the molecular model and the simulation method are described. Thereafter, the simulation results are presented, compared with the experimental values, and discussed.

Molecular Model

PVC and PVA are modeled as CH_3-$(CHCl\text{-}CH_2)_{50}$-$CHCl\text{-}CH_3$ and CH_3-$(CHOH\text{-}CH_2)_{34}$-$CHOH\text{-}CH_3$ respectively, and the configuration of polymer is assumed to be head-to-tail junctions and syndiotatic in which racemic dyad is connected along the chain. We choose to make both groups before and behind the center site of polymer equivalent and to terminate CH_3 group on both terminal sites. CH_3 and CH_2 groups are considered as single interaction pseudo-atoms located at centers of carbon atoms. The nonbonded interaction between i site and j site is calculated by Coulombic and Lennard-Jones (LJ) potential:

$$u_{ij} = \frac{q_i q_j e^2}{r_{ij}} + 4\varepsilon_{ij}\left[\left(\frac{\sigma_{ij}}{r_{ij}}\right)^{12} - \left(\frac{\sigma_{ij}}{r_{ij}}\right)^{6}\right] \quad (1)$$

where r_{ij} is the distance between i site and j site, q_i is a partial charge located at i site, and e is the electronic charge. ε_{ij} and σ_{ij} are obtained using the standard Lorentz-Berthelot combining rules given by

$$\sigma_{ij} = 0.5(\sigma_i + \sigma_j) \text{ and } \varepsilon_{ij} = \sqrt{\varepsilon_i \varepsilon_j}. \quad (2)$$

In the same molecule, the nonbonded potential between sites by three or more than three bonds is calculated. In addition to LJ and Coulombic interaction, the torsional energy of molecule is taken into account with eqs. (3) and (4) for PVC[25] and PVA,[26] respectively.

$$u_t = \frac{1}{2}B_1(1 - \cos\phi) + \frac{1}{2}B_2(1 - \cos 3\phi) \quad (3)$$

$$u_t = \frac{1}{2}k_\phi(1 - \cos 3(\phi - \delta)) \quad (4)$$

where B_1, B_2, k_ϕ, δ are parameters, ϕ is dihedral angle. In eq. (4), the *cis* conformation corresponds to $\phi = 0°$. The LJ parameter and the partial charge of site, bond angle, bond length, the parameters for torsional energy are summarized in Table I and Table II. The partial charges of CH_3, CH_2, and H sites of PVC are assumed to be zero because these sites are included in the nonpolar backbone. And the partial charge of chlorine site is adopted with -0.1987, which is not greatly different from that[28] of chlorine site in CH_3Cl molecule. The partial charge of the methine carbon atom is determined by the electroneutrality of molecule. The bond angle and bond length are fixed in simulation.

Table I. Potential and Geometric Parameter for PVC. k is Boltzmann Constant

Site	σ (nm)[a]	ε/k (K)[a]	q (e)[c]
CH_3	0.37197	71.439	0
CH_2	0.393[b]	45.8[b]	0
Methine C	0.34921	27.186	0.1987
Cl	0.35386	80.954	-0.1987[a]
H	0.28621	4.330	0
Bond Length (nm)[d]		Bond Angle (degree)[d]	
C-C	0.153	∠CCC	112[e] and 115.5[f]
C-H	0.109	∠CCH	110.7
C-Cl	0.183	∠CCCl	109.7
Torsion[g]	B_1 (kJ/mol)	B_2 (kJ/mol)	
C-C-C-C	2.092	5.8576	

[a]From ref. 4. [b]From ref. 27. [c]Modified. [d]From ref. 25. [e]Methine carbon centered. [f]Methylene carbon centered. [g]Backbone torsion within a racemic dyad in ref. 25.

Table II. Potential and Geometric Parameter for PVA.[a] H(O) is Hydrogen Atom Next to Oxygen Atom

Site	σ (nm)	ε/k (K)	q (e)
CH_3	0.37197[b]	71.439[b]	0
CH_2	0.393[c]	45.8[c]	0
Methine C	0.34921[b]	40.43	0.3
O	0.317	78.213	-0.7
H	0.257	25.269	0
H(O)	0	0	0.4
Bond Length (nm)		Bond Angle (degree)	
C-C	0.153	∠CCC	109.45
C-H	0.109[d]	∠CCH	110
C-O	0.1431	∠CCO	107.8
O-H	0.097	∠COH	105
Torsion	δ (degree)	k_ϕ (kJ/mol)	
H-O-C-C	180	6	
C-C-C-C	180	11.5	
C-C-C-H	180	11.5	

[a]From ref. 26. [b]From ref. 4. [c]From ref. 27. [d]From ref. 25.

Simulation Method

All simulations are performed for a total of 10 and 12 molecules in cubic simulation box for PVC and PVA, respectively, and three dimensional periodic boundary conditions are used. The types of Monte Carlo moves are as follows: (a) CBMC move, (b) CONROT move, (c) reptation, (d) volume fluctuation in the NPT ensemble.

In move (a), a molecule is selected at random and whether to regrow toward the chain start or the chain end is chosen randomly. Then the molecule is cut at a randomly selected

backbone site among the first four sites or the last four sites in backbone, which is reasonable because the regrowing of more than four sites would be nearly not successful. Regrowing begins at the cut site of backbone. The number of trial orientations per the site of backbone is fixed at 10. At a branch point, all the sites next to the branch point are attached simultaneously. That is, methine hydrogen atom, CH_2 group, chlorine atom for PVC, and methine hydrogen atom, CH_2 group, oxygen atom for PVA are attached at the methine carbon atom simultaneously. The position of hydrogen atom next to oxygen atom in PVA is determined by selecting randomly a torsional angle around the C-O bond. The regrowth is accepted with probability as following equation.[29]

$$acc(m \rightarrow n) = \min\left[1, \prod_{j=1}^{l} W_j^{(n)} \Big/ \prod_{j=1}^{l} W_j^{(m)}\right] \quad (5)$$

$$W_j^{(n)} = \sum_{i=1}^{t} \exp(-\beta u_i^{(n)}) \text{ and } W_j^{(m)} = \sum_{i=1}^{t} \exp(-\beta u_i^{(m)}) \quad (6)$$

where $W_j^{(n)}$ and $W_j^{(m)}$ are the new and the old j Rosenbluth factor respectively. j is the growth step, l the total number of growth steps, i a particular trial, t the number of trials, u_i the total energy for i trial. β is $1/kT$, where k is Boltzmann constant and T is temperature. In move (b), the method in ref. 17 and 18 are mainly used. The first three backbone sites and the last three backbone sites do not move in this move, but move in CBMC move. First, the driver site is selected at random, and the driver angle is determined by $\varphi^{(n)} = \varphi^{(m)} + \Delta\varphi$ in which $\Delta\varphi$ is randomly selected between -10° and 10°. $\varphi^{(n)}$ and $\varphi^{(m)}$ are the new and the old driver angles respectively. After the new position of driver site is determined by $\varphi^{(n)}$, the trimer next to driver site toward the end of chain is cut. Then all the geometrical solutions of rebridged trimers are found, and the new positions of side sites are calculated from each rebridged trimers. For PVA, the hydrogen atom connected to oxygen atom is built by selecting randomly a torsional angle around the C-O bond. The new Rosenbluth factor, $W^{(n)}$, is calculated as follows;

$$W^{(n)} = \sum_{i=1}^{k(n)} J_i^{(n)} \exp(-\beta u_i^{(n)}) \quad (7)$$

where $k(n)$ is the number of geometrical solutions found, $J_i^{(n)}$ is Jacobian factor of i trial, and $u_i^{(n)}$ is the total energy for i trial. The old Rosenbluth factor, $W^{(m)}$, is calculated in the same way as ref. 17, and the attempted move is accepted with the probability,

$$acc(m \rightarrow n) = \min\left[1, W^{(n)}/W^{(m)}\right] \quad (8)$$

In move (c), it is chosen randomly whether the tail is the chain start or the chain end. Then the 8 sites and 10 sites of the tail in PVC and PVA molecule respectively are erased, and those sites erased are randomly attached at the head as shown in Figure 1. The position of hydrogen atom next to oxygen atom in PVA is determined by selecting randomly a torsional angle around the C-O bond. The move is accepted with probability,

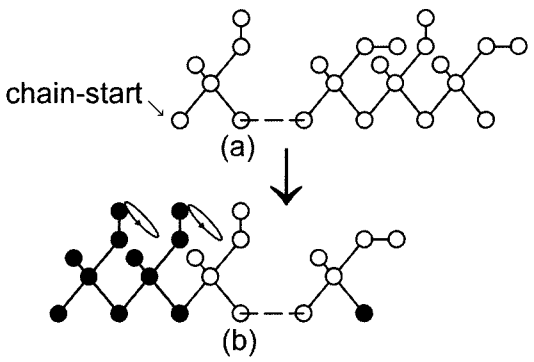

Figure 1. Schematic of a reptation move for PVA molecule before (a) and after (b) move, respectively, when the chain start is the head. The closed circle denotes the site whose position or species are changed after move.

$$acc(m \rightarrow n) = \min[1, \exp(-\beta \Delta u)] \quad (9)$$

where Δu is the energy change for the trial move. In move(d), volume fluctuation[30] is attempted by randomly changing all edge lengths of the simulation box.

Configuration in simulation is generated by a randomly selected MC move. The MC move occurs with the following probabilities: 6%, 80%, and 14% for move (a), (b), and (c) respectively in NVT simulation, and 6%, 80%, 10%, and 4% for move (a), (b), (c), and (d) respectively in NPT simulation. The maximum change of edge length of the simulation box in move (d) is adjusted to give an average acceptance ratio of 40% every 25000 configurations. In general, a part potential with a spherical cutoff is used to reduce the computing time in computer simulation. For the LJ part of the potential, the cutoff distance is 1 nm, and the potential arising from truncation is corrected. However we do not consider the Coulombic potential with a spherical cutoff and its correction. Instead we calculate the Coulombic potential of a site with all the sites in simulation box, by which the incorrectness of calculation causing from the electrical unneutrality in space within cutoff distance can be avoided.

The initial configurations are generated as follows: All molecules are randomly grown site by site in the simulation box that has a volume of approximately 5 times the experimental value. If a adding site overlaps severely with other sites in the simulation box, the site is rejected. Then compressing process composed of numbers of stage is performed, in which the size of the simulation box decreases gradually until the density is close to the experimental one. At each of the compressing stage, the move (a), (b), and (c) occur with probability of 6%, 80%, and 14% respectively. Each move is accepted only if the potential of the new con-

figuration is lower than the old one for the energy minimization. The number of configurations generated at each of the compressing stage is 7.5×10^5 to 1.5×10^6. In the compressing process, we often increase the size of the simulation box in order to avoid trapping of sites in local regions of high density during simulation, in which the system is energy minimized with only the repulsive r^{-12} part of LJ energy instead of the full energy by eq. (1). Finally the NVT MC is performed with a large number of MC cycles, followed by NPT MC. In NPT MC simulation, the number of configurations generated in equilibration run is 2.5×10^6 and 2×10^6 for PVC and PVA, respectively, and that in equilibrium run is 3×10^6 and 2.5×10^6 for PVC and PVA, respectively.

Results and Discussion

To test the effects of smaller simulation runs on the calculated results, the density of PVC was calculated with 2.5×10^6 and 2.5×10^6 configurations in equilibration run and equilibrium run respectively at 456 K, and the density of PVA was calculated with 2×10^6 and 2×10^6 configurations in equilibration run and equilibrium run respectively at 440 K. These densities of PVC and PVA are equal to the simulation results in Table III, indicating the numbers of configurations generated in equilibration run and equilibrium run are large enough in this study.

Table III shows that the calculated density decreases as temperature increases, which is consistent with the experimental trend for PVC and PVA. However, the calculated densities almost lie about 15% below the experimental values, and the calculated density of PVA at 510 K is lower 7% than the experimental one. In fact the density of polymer system is somewhat different on tacticity. For example, Rosa and co-worker[7] reported that the calculated densities of PVA were 1.14 and 1.21 gcm^{-3} for syndiotactic and isotactic polymer respectively, and that the solubility parameter and the hydrogen bonds amounts for PVA system were influenced by tacticity. Therefore, the calculated densities in this study cannot be exactly compared with the experimental values. The discrepancy between the simulated and the experimental density greatly occurs when the molecular weight of model polymer in simulation is very low. The calculated density of *cis*-1,4 polyisoprene,[23] for instance, increased as the chain length increased, and agreed with the experimental one at high enough chain lengths.

Table III shows the mean square backbone end-to-end distance, $\langle R^2 \rangle$, and the mean square radius of gyration, $\langle S^2 \rangle$, for PVC and PVA at 0.1 MPa by eqs. (10) and (11), respectively.

$$\langle R^2 \rangle = \langle (\boldsymbol{r}_1 - \boldsymbol{r}_t)^2 \rangle \tag{10}$$

$$\langle S^2 \rangle = \langle \sum_{i=1}^{n_t} (\boldsymbol{r}_i - \boldsymbol{r}_{com})^2 \rangle \tag{11}$$

where $\boldsymbol{r}_1$ and $\boldsymbol{r}_t$ are the position vectors of the first and the last CH_3 groups of chain. n_t is the total number of sites in backbone of the chain, and $\boldsymbol{r}_{com}$ is the position vector of the center-of-mass of the chain. The distance between the two terminal CH_3 groups is larger at higher temperature for PVC, which is probably due to that the motions of skeletal chain increase with increasing temperature. $\langle S^2 \rangle$ of PVC would be not greatly dependent on the partial charge of polymer. This is can be explained from ref. 4, in which $\langle S^2 \rangle$ of PVC with partial charge is similar to that without charge. However, Yoon and co-workers[2] reported that $\langle R^2 \rangle$ was influenced by the intermolecular Coulombic interaction for PVC. The difference in partial charges has a minor effect on chain dimension in general.[1] As shown in Table III, $\langle R^2 \rangle$ and $\langle S^2 \rangle$ of PVC change strongly with increasing temperature, whereas those of PVA are nearly not dependent on temperature. This difference between PVC and PVA results probably from two factors. One of them is that the free vol-

Table III. The Calculated Density, the Mean Square Backbone End-to-End Distance $\langle R^2 \rangle$, and the Mean Square Radius of Gyration $\langle S^2 \rangle$ for PVC and PVA at 0.1 MPa. Densities in Parentheses are Experimental Values[31]

Polymer	Temperature (K)	Density (gcm^{-3})	$\langle R^2 \rangle$ (nm^2)	$\langle S^2 \rangle$ (nm^2)
PVC	373	1.13 (1.35)	12.90	1.62
PVC	456	1.10 (1.28)	15.90	1.67
PVC	500	1.04 (1.23)	17.50	1.77
PVA	377	1.11 (1.30)	6.57	1.01
PVA	440	1.07 (1.24)	6.57	1.02
PVA	510	1.08 (1.16)	6.50	1.01

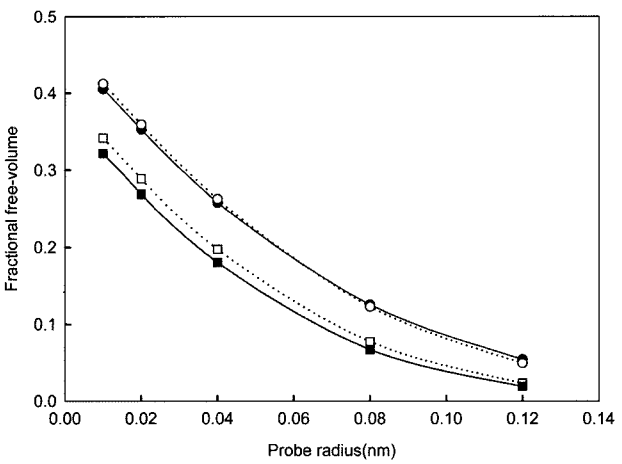

Figure 2. Fractional free-volume as a function of the probe size at 0.1 MPa: PVC at 373 K (closed circle), PVC at 456 K (open circle), PVA at 377 K (closed square), and PVA at 440 K (open square).

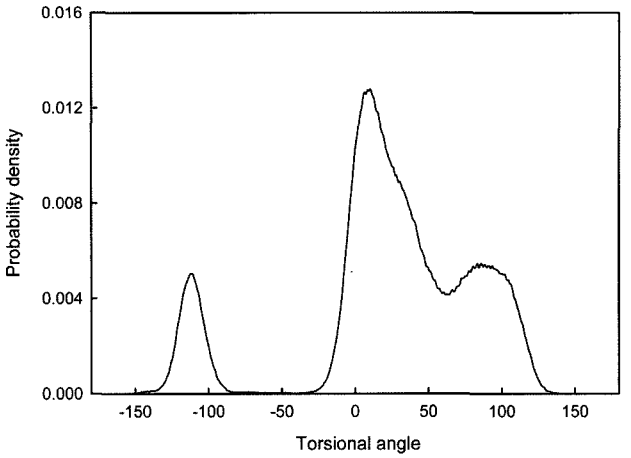

Figure 3. Distribution of torsional angles of PVC at 373 K.

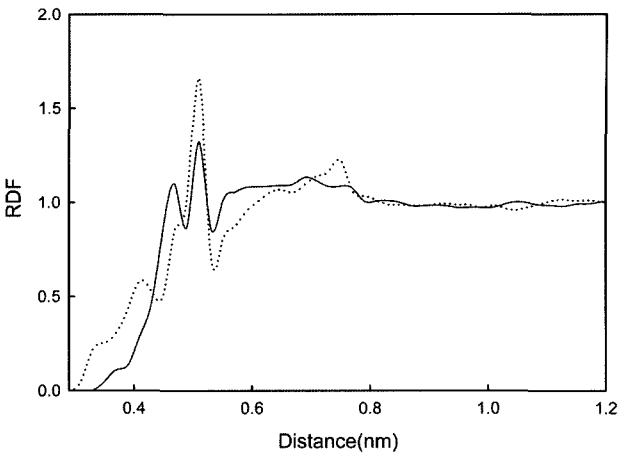

Figure 4. Radial distribution function (RDF) in PVC system at 0.1 MPa and 373 K: methine carbon - methine carbon (solid line) and methylene group - methylene group (dotted line).

ume of PVC is larger. The other reason is that the binding interactions of sites of PVC with their environment are smaller. Therefore the motion of skeletal chain is easier for PVC than for PVA.

Free volume distribution is important on the properties of amorphous polymers. Figure 2 shows the fractional free-volume distribution as a function of the probe size for PVC and PVA by simulation. Details of the procedure are given in ref. 32. In this study, the probe was allowed to scan uniform grid whose the gridlines are spaced by about 0.02 nm. Each site was assigned an effective radius equaling the sum of half σ of site and the probe radius, and subcells whose centers lay within the effective radius of any site were assumed to be occupied. The total fractional free-volume is smaller for PVA than for PVC. This reason seems that oxygen atom which is smaller than chlorine atom acts more effectively in packing with the other sites of polymer.

The distribution of torsional angles of syndiotactic PVC at 373 K is shown in Figure 3, which is largely different from that of atactic PVC.[2] The plus sign of the torsional angle denotes *g* configuration (*trans* being 0). The distributions of torsional angles at 456 K and 500 K are quite similar to those at 373 K for PVC. The very low probability density in the angle range from -140° to -180° and from 140° to 180° are mainly due to that the two backbone carbons separated by three bonds have influence on torsional rotational barriers. And the very low probability density in the angle range from -40° to -80° is mainly due to influence of the backbone carbon and chlorine atom separated by three bonds on torsional rotational barriers.

The solubility constant of a small molecule is mostly calculated with Widom method:[33]

$$H = \frac{T_s}{P_s T} \frac{<V\exp(-\beta\Delta u)>_{NPT}}{<V>_{NPT}} \quad (12)$$

where $T_s = 273.15$ K and $P_s = 1.013$ bar. T is temperature, V is the volume of the system, and <···> is ensemble average. Δu is potential calculated by random insertion of the ghost molecule in the polymer system. Table IV shows the solubility constant with Widom method. The potential parameter of ghost molecule are given elsewhere.[5] Table IV shows that the solubility constant obviously decreases with increasing temperature. For each of permeant molecule, the solubility constant in PVC is similar to that in PVA at the higher temperature (approximately 500 K). However it is remarkable that the solubility constants of CH_4, O_2, and Ar in PVA at 377 K are larger by about 2 times than those in PVC at 373 K.

Figures 4 and 5 show the radial distribution functions

Table IV. The Calculated Solubility Constant of Permeant Molecule in PVC and PVA at 0.1 MPa

Polymer	Temperature (K)	Solubility Constant ($cm^3(STP)cm^{-3}bar^{-1}$)					
		CH_4	N_2	O_2	Ar	H_2	He
PVC	373	0.736	0.319	0.404	0.456	0.153	0.121
PVC	456	0.321	0.169	0.209	0.237	0.110	0.101
PVC	500	0.276	0.164	0.195	0.215	0.117	0.111
PVA	377	1.800	0.455	0.704	0.860	0.139	0.085
PVA	440	0.603	0.228	0.316	0.383	0.100	0.074
PVA	510	0.286	0.119	0.163	0.187	0.065	0.056

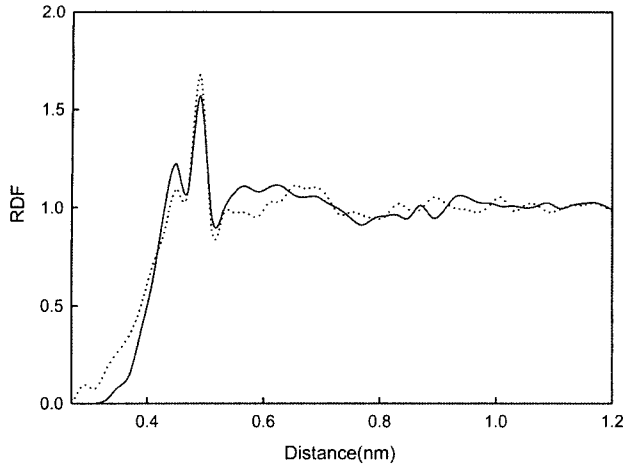

Figure 5. Radial distribution function (RDF) in PVA system at 0.1 MPa and 440 K: methine carbon - methine carbon (solid line) and methylene group - methylene group (dotted line).

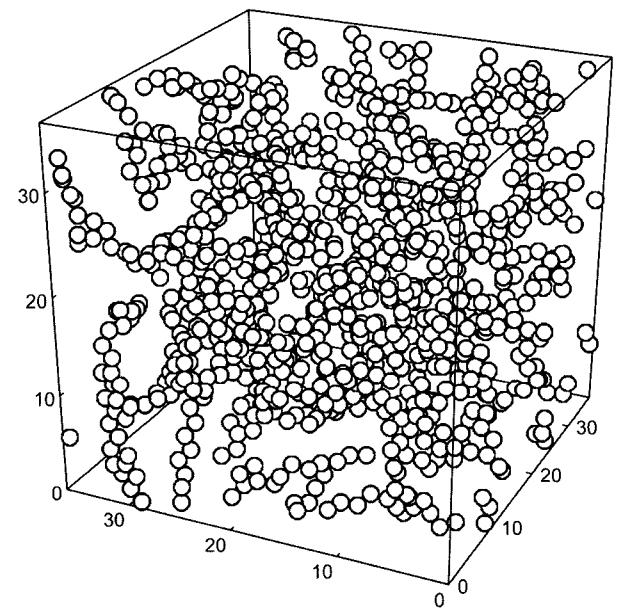

Figure 6. Snap shot for the configuration of PVC system at 0.1 MPa and 373 K. Open circle is methyl or methylene group, or methine carbon atom. Chlorine atom and methine hydrogen atom were omitted for clarity.

(RDFs) of methine carbon-methine carbon and CH_2 group-CH_2 group in the PVC system at 373 K and the PVA system at 440 K, respectively. Because the angular distributions were not calculated in this study, the orientational informations were not given in RDFs. The RDFs in the PVC system at 456 K and 500 K were very similar to those at 373 K. Also the RDFs in PVA system were very similar at 377 K, 440 K, and 510 K. It seems that the peaks of methine carbon-methine carbon located at nearly 0.45 and 0.5 nm result

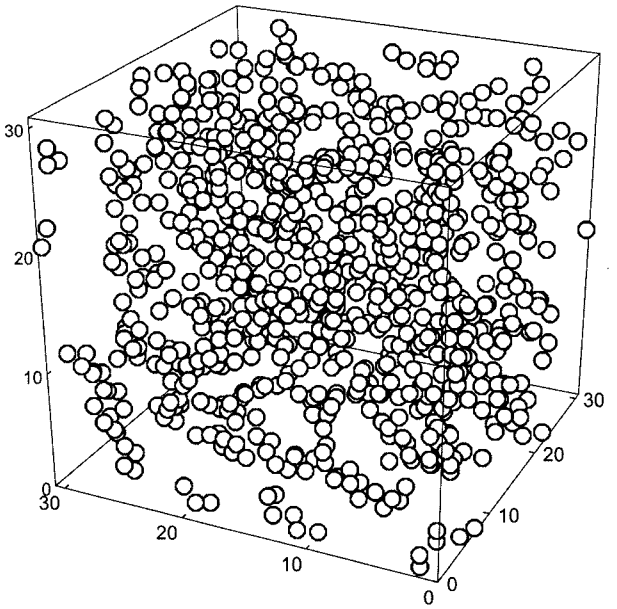

Figure 7. Snap shot for the configuration of PVA system at 0.1 MPa and 440 K. Open circle is methyl or methylene group, or methine carbon atom, oxygen atom, hydrogen atom neighboring oxygen, and methine hydrogen atom were omitted for clarity.

mainly from the contribution of the intramolecular pair for PVC and PVA. Similarly, the peaks of CH_2 group-CH_2 group located at nearly 0.5 nm are probably due to a large contribution of the intramolecular pair for PVC and PVA. Figures 6 and 7 show the snap shot for the configuration of PVC and PVA system, respectively.

Acknowledgement. This work was supported by Pukyong National University Research Fund in 2002.

References

(1) G. Tanaka and W. L. Mattice, *Macromolecules*, **28**, 1049 (1995).
(2) G. D. Smith, R. L. Jaffe, and D. Y. Yoon, *Macromolecules*, **26**, 298 (1993).
(3) I. Neelov, S. Niemela, and F. Sundholm, *J. Non-Cryst. Solids*, **235-237**, 340 (1998).
(4) S. Neyertz, D. Brown, and J. H. R. Clarke, *J. Chem. Phys.*, **105**, 2076 (1996).
(5) N. F. A. van der Vegt, *J. Membr. Sci.*, **205**, 125 (2002).
(6) G. E. Karlsson, T. S. Johansson, U. W. Gedde, and M. S. Hedenqvist, *J. Macromol. Sci.-Phys.*, **B41**, 185 (2002).
(7) A. De La Rosa, L. Heux, J. Y. Cavaille, and K. Mazeau, *Polymer*, **43**, 5665 (2002).
(8) F. Muller-Plathe, *J. Chem. Phys.*, **108**, 8252 (1998).
(9) F. Muller-Plathe, *J. Membr. Sci.*, **141**, 147 (1998).
(10) Y. Tamai and H. Tanaka, *Chem. Phys. Lett.*, **285**, 127 (1998).
(11) D. Hofmann, L. Fritz, J. Ulbrich, C. Schepers, and M. Bohning, *Macromol. Theory Simul.*, **9**, 293(2000).

(12) G. E. Karlsson, U. W. Gedde, and M. S. Hedenqvist, *Polymer*, **45**, 3893 (2004).
(13) S. S. Jawalkar, S. G. Adoor, M. Sairam, M. N. Nadagouda, and T. M. Aminabhavi, *J. Phys. Chem. B*, **109**, 15611 (2005).
(14) D. Frenkel, G. C. A. M. Mooij, and B. Smit, *J. Phys.: Condensed Matter*, **4**, 3053(1992).
(15) M. Laso, J. J. de Pablo, and U. W. Suter, *J. Chem. Phys.*, **97**, 2817 (1992).
(16) L. R. Dodd, T. D. Boone, and D. N. Theodorou, *Mol. Phys.*, **78**, 961(1993).
(17) M. G. Wu and M. W. Deem, *Mol. Phys.*, **97**, 559 (1999).
(18) V. G. Mavrantzas, T. D. Boone, E. Zervopoulou, and D. N. Theodorou, *Macromolecules*, **32**, 5072 (1999).
(19) P. V. K. Pant and D. N. Theodorou, *Macromolecules*, **28**, 7224 (1995).
(20) N. C. Karayiannis, V. G. Mavrantzas, and D. N. Theodorou, *Phys. Rev. Lett.*, **88**, 105503 (2002).
(21) N. C. Karayiannis, A. E. Giannousaki, V. G. Mavrantzas, and D. N. Theodorou, *J. Chem. Phys.*, **117**, 5465 (2002).
(22) R. Faller, F. Muller-Plathe, M. Doxastakis, and D. Theodorou, *Macromolecules*, **34**, 1436 (2001).
(23) M. Doxastakis, V. G. Mavrantzas, and D. N. Theodorou, *J. Chem. Phys.*, **115**, 11339 (2001).
(24) P. Gestoso, E. Nicol, M. Doxastakis, and D. N. Theodorou, *Macromolecules*, **36**, 6925 (2003).
(25) G. D. Smith, P. J. Ludovice, R. L. Jaffe, and D. Y. Yoon, *J. Phys. Chem.*, **99**, 164 (1995).
(26) F. Muller-Plathe and W. F. van Gunsteren, *Polymer*, **38**, 2259 (1997).
(27) E. Zervopoulou, V. G. Mavrantzas, and D. N. Theodorou, *J. Chem. Phys.*, **115**, 2860 (2001).
(28) B. J. C. Cabral, J. L. Rivail, and B. Bigot, *J. Chem. Phys.*, **86**, 1467 (1987).
(29) M. G. Martin and J. I. Siepmann, *J. Phys. Chem. B*, **103**, 4508 (1999).
(30) M. P. Allen and D. J. Tildesley, in *Computer Simulation of Liquids*, Clarendon, Oxford, 1987.
(31) P. Zoller and D. J. Walsh, in *Standard Pressure-Volume-Temperature Data for Polymers*, Technomic, Lancaster, 1995.
(32) S. Misra and W. L. Mattice, *Macromolecules*, **26**, 7274 (1993).
(33) N. F. A. van der Vegt, W. J. Briels, M. Wessling, and H. Strathmann, *J. Chem. Phys.*, **105**, 8849 (1996).